Decision Tree-Based Smart Clothing in Enhancing the Psychological Care Effect of Medical Humanities Education

Jiankun Ren
School of Nursing, Hebi Polytechnic, Hebi 458030, Henan Province, China
Corresponding author: Jiankun Ren (e-mail: hlxyrjl1982@163.com)

ABSTRACT This study presents a smart textile system integrating an improved C4.5 decision tree for real-time identification and personalized intervention of medical students' psychological states in medical humanities education. The system acquires multimodal physiological signals, including heart rate variability and electrodermal activity, through flexible textile sensors, and extracts temporal and nonlinear features for high-dimensional analysis. A dynamically weighted hybrid splitting criterion combining Information Gain Ratio and Gini index enhances classification accuracy and interpretability. The framework implements a closed-loop perception–decision–intervention mechanism, delivering targeted tactile feedback to regulate sympathetic–parasympathetic balance. Experimental results show recognition accuracies of 93.5% in end-of-life care and 91.8% in difficult diagnosis scenarios, with LF/HF ratio reductions of up to 46.6% and strong correlation with self-reported anxiety (R^2=0.78). The approach is applicable to wearable sensing and edge-computing frameworks, leveraging real-time physiological signal acquisition and adaptive feedback. This provides a practical engineering solution for objective, timely, and quantifiable psychological care, bridging intelligent human–machine interaction with principles relevant to signal processing and embedded decision systems.

INDEX TERMS smart textiles, decision tree, physiological signal processing, edge-computing frameworks

I. INTRODUCTION

MEDICAL humanities education is a fundamental aspect of developing medical students' empathy, communication, and professional ethics, and its effectiveness is a direct reflection of quality medical practice and effective doctor-patient relationships. Within the context of highly contextualized and emotional simulation training or clinical practice, students' psychological fluctuations affect students' capacity to acquire and internalize humanistic traits [1,2]. Therefore, it is of urgent and significant importance to examine how to understand and support students' psychological activities throughout students' learning processes when exploring their effectiveness of medical humanities education [3-5].

Psychological support methods in medical humanities training are encountering various bottlenecks. Educators primarily rely on post-hoc interviews and self-report measure scales - both of which rely on subjective, retrospective data and cannot detect instantaneous or implicit psychological variability that occurs during the actual teaching experience [6,7]. Episodes of intense role-play or ethical discussions lead to acute stress or empathy challenges, but these internal experiences cannot be well-observed during professional performance [8,9]. Consequently, the educator has no objective, continuous evidence with which to assess the emotional variability of students, and interventions are typically delivered in the form of generalized group counselling or delayed one-to-one support provided weeks after the training., and not typically personalized or contemporary, nor precise.

In response to these challenges, existing work has tried to incorporate some kind of technological strategies. Some researchers have sought to analyze the emotions inferred from facial expressions or tone of voice captured in video recordings; however, these types of procedures are easily limited by individuals' habitual expressions and scene rules, often failing to produce sufficiently valid and reliable data, particularly in medical contexts where a professional demeanor is expected [10,11]. Smart textile-based wearables, in contrast, offer a less obtrusive means of signal acquisition, leveraging the natural integration of sensors into garments to capture single physiological signals (i.e. heart rate) over time; however, single indicators often do not reliably differentiate complex psychological constructs as in when investigating constructs such as empathy and anxiety [12,13]. In addition, prior analyses on physiological data have often employed conventional machine learning models. When utilizing multi-dimensional physiology in the data, these analyses will become "black boxes" due to complexity which diminishes insight into the intended educational intervention or to use models without feature selection capabilities which limit the accuracy to identify aspects of key states [14,15]. Overall, within this context of medical humanities, existing work has yet to investigate a real-time awareness and perception solution to monitor psychological states which will deeply fuse multi-source objective data while having both high accuracy and good interpretability and would fit seamlessly into the normal health professions' educational processes.

In response to the pressures inferred by the inadequate use of multimodal data, and challenges arising from balancing model interpretability and accuracy in medical humanities education leading to ineffective psychological care, the current study proposes an intelligent clothing system built around an enhanced decision tree approach. This approach first uses customized smart clothing to collect multimodal physiological data streams simultaneously with a primary focus on heart rate variability and skin conductance. In the data processing phase, temporal and nonlinear features are extracted to construct a high-dimensional feature space. The core contribution of the proposed model formation is dynamically weighted hybrid splitting criterion using information gain ratio and Gini, which is embedded into the C4.5 decision tree growth process to guide the growth process to preferentially choose the most discriminatory and statistically significant physiological features to split at each node that produces a streamlined classification model to develop clear discrimination rules. The classification model uses physiological signals of continuous streams of data to categorize into discrete psychological states. From those classifications, the system triggers specific tactile feedback patterns that were built into the clothing to develop a closed-loop intervention and system. This study provides a new technical path and the base theory to use to create non-invasive and objective psychological care within medical humanities education.

II. CONSTRUCTION OF A DECISION TREE-BASED INTELLIGENT CLOTHING SYSTEM

This chapter focuses on how to deeply integrate decision tree algorithms with smart clothing hardware to construct a closed-loop psychological care system for practical scenarios in medical humanities education. Unlike pure algorithm research or hardware research, this study emphasizes the collaborative design and systematic integration of algorithms and hardware, aiming to achieve a complete application loop from physiological signal perception and psychological state recognition to real-time tactile intervention, highlighting its usability, interpretability, and practicality in real teaching environments.

A. SYSTEM OVERALL ARCHITECTURE

To achieve real-time perception and precise intervention of the psychological state of students in medical humanities education, this study designed and implemented a hierarchical intelligent system based on a decision tree model. This system integrates smart clothing, edge computing, and interaction logic into a complete automated loop of 'perception, decision-making, and intervention.' Its overall architecture is shown in Figure 1.

Figure 1 illustrates that the architecture consists of three functionally defined and collaborative logical layers. The physiological data perception layer uses a garment-based sensing platform as its physical carrier, wherein flexible textile electrodes and conductive yarns are seamlessly woven into the fabric, continuously collecting the wearer's raw electrocardiogram (ECG) and skin conductance signals through its integrated flexible textile electrodes and micro-sensor modules [16,17]. The edge computing and decision-making layer, as the core of the system, is deployed on an embedded hardware platform; this layer receives raw data from the perception layer, performs signal preprocessing and feature extraction, and inputs the obtained multimodal physiological feature vectors into a pre-trained improved C4.5 decision tree model to complete the real-time classification and recognition of specific psychological states. The humanistic care interaction layer, based on the output of the decision-making layer, calls the preset intervention strategy and drives the tactile feedback elements integrated on the clothing to generate customized vibration patterns, thereby forming a closed-loop intervention. The layers interact with each other through wireless and wired communication protocols to ensure the continuity and timeliness of system operation. Real-time Intervention Design: The term 'real-time' in this pedagogical context refers to near-real-time responsiveness sufficient for modulating sustained psychological states during a training scenario (typically lasting minutes), rather than requiring millisecond-level reflexes. To balance algorithmic complexity (e.g., FFT for HRV) with responsiveness, the system employs a sliding window mechanism for feature computation and state classification. This design ensures periodic state updates and intervention triggers within a timeframe that is meaningful for educational interaction.

B. MULTIMODAL PHYSIOLOGICAL DATA ACQUISITION AND PREPROCESSING

This study used a custom smart garment featuring knitted silver-coated nylon electrodes and a textile-based conductive grid for signal acquisition to collect multimodal physiological signals. The platform integrates a single-lead textile electrode and a bipolar constant-voltage skin conductance sensor, which simultaneously acquires raw electrocardiogram (ECG) signals and skin conductance signals at sampling frequencies of 256 Hz and 32 Hz, respectively. To mitigate motion artifacts—a critical challenge for textile electrodes during role-play activities—the garment incorporates an ergonomic design with snug-fitting cuffs and chest bands to maintain consistent electrode-skin contact. The analog front-end includes hardware filters (bandpass for ECG, low-pass for EDA) and a driven-right-leg circuit

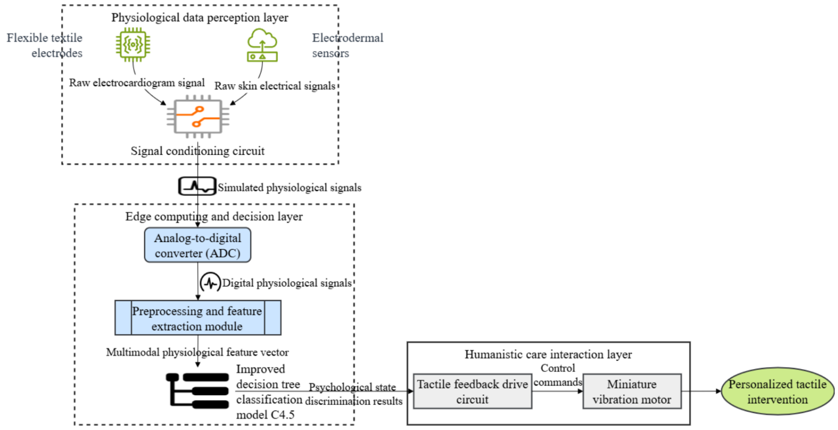

FIGURE 1. Overall framework of the smart-textile-based psychological state perception and intervention system

to suppress common-mode interference. Furthermore, the raw signals are monitored in real-time for saturation or abrupt baseline shifts indicative of severe motion; data segments contaminated by such artifacts are flagged and excluded from immediate feature extraction, relying instead on interpolation from adjacent clean segments for short gaps (<5s). The raw signals are amplified and primary filtered by a built-in low-noise analog front end, and then wirelessly transmitted to the edge computing unit via Bluetooth 5.0. Signal preprocessing aims to suppress noise and extract discriminative features. The ECG signal is first passed through a bandpass filter with a cutoff frequency of 0.5 Hz to 35 Hz to eliminate baseline drift and power line interference. Then, the Pan-Tompkins algorithm is used to detect the R-wave peak value, and a series of continuous heartbeat intervals are calculated accordingly [18,19]. The skin conductance signal is passed through a low-pass filter with a cutoff frequency of 1 Hz to separate the slowly changing skin conductance level components, and its rapidly changing skin conductance response peak value is further detected. Based on the preprocessed signal, this study extracted key temporal and nonlinear features characterizing the activity of the autonomic nervous system. For the intercardiac interval sequence, its mean and standard deviation were calculated, and the power spectral density was estimated using fast Fourier transform, extracting the ratio of low-frequency power (LF) to high-frequency power (HF) [20,21]. The equation for calculating this ratio is:

$$\mathrm{LF}/\mathrm{HF} = \frac{P_{LF}}{P_{HF}} \tag{1}$$

P_{LF} represents the power in the 0.04 Hz to 0.15 Hz frequency band, which is related to the joint regulation of the sympathetic and vagus nerves; P_{HF} represents the power in the 0.15 Hz to 0.4 Hz frequency band, mainly reflecting vagal nerve activity. This ratio is a core indicator for assessing autonomic balance and psychological stress state. It should be noted that while the LF/HF ratio is widely used as an indicator of sympathovagal balance, its interpretation should be considered alongside absolute power values to avoid misleading conclusions when total power varies significantly. In this study, we report both the ratio and the absolute HF power change to provide a more comprehensive assessment of autonomic nervous system activity.

For skin conductance signals, the mean of skin conductance level signals, the number of skin conductance response peaks, and their average amplitude were extracted. Finally, all these features were combined into a comprehensive multimodal physiological feature vector for subsequent model training and inference. The definitions and physiological meanings of all features are shown in Table 1.

Table 1 systematically defines six core physiological features extracted from heart rate variability and electrodermal activity (EDA), which quantify the activity state of the autonomic nervous system in both the time and frequency domains. Heart rate variability primarily reflects changes in cardiac rhythm, with the LF/HF ratio being a key indicator for assessing sympathetic-vagal balance [22,23]. EDA directly characterizes changes in sympathetic-driven skin electrical secretion, and the number and amplitude of peak values are sensitive parameters for measuring psychological arousal. The combination of these features provides an objective, multimodal physiological basis for subsequent decision tree models to distinguish different psychological states.

C. IMPROVED CONSTRUCTION AND TRAINING OF DECISION TREE MODEL

Based on the preprocessed multimodal physiological feature vectors, this study constructs an improved decision tree model to achieve accurate classification of psychological states. The core innovation of this model lies in applying a dynamically weighted hybrid splitting criterion to replace the traditional C4.5 algorithm's single-dependency information gain ratio node splitting strategy [24,25]. For any node S to be split and feature A, the criterion first calculates its information gain ratio $\mathrm{GainRatio}(S, A)$ and Gini index decrease $\Delta\mathrm{Gini}(S, A)$, respectively [26,27]. Information gain ratio:

TABLE 1. Multimodal physiological characteristics

Modal name	Feature	Calculation formula / definition	Physiological meaning
Heart rate variability	Mean heartbeat interval	$\text{MeanNN} = \frac{1}{N}\sum_{i=1}^{N} NN_i$	Reflects average heart rate level
Heart rate variability	Standard deviation of cardiac interval	$\text{SDNN} = \sqrt{\frac{1}{N-1}\sum_{i=1}^{N}(NN_i - \text{MeanNN})^2}$	Reflects overall autonomic nervous system activity
Heart rate variability	LF/HF ratio	$\text{LF/HF} = P_{LF}/P_{HF}$	Characterizes the sympathetic-vagal balance; elevated values indicate increased stress
Skin electrical activity	Average skin conductivity	$\text{MeanSCL} = \frac{1}{T}\sum_{t=1}^{T} SCL_t$	Baseline reflecting slow changes in arousal
Skin electrical activity	Peak number of skin conductance response	NSSCR (Number of Specific Skin Conductance Responses): Number of peak values with amplitudes exceeding $0.01\ \mu$S within the time window	Indicator of the instantaneous excitation frequency of the sympathetic nervous system
Skin electrical activity	Average amplitude of skin conductance response	$\text{MeanAmpSCR} = \frac{1}{\text{NSSCR}}\sum_{j=1}^{\text{NSSCR}} \text{AmpSCR}_j$	Reflecting the intensity of a single excitation event

$$\text{GainRatio}(S,A) = \frac{\text{IG}(S,A)}{\text{SplitInfo}(S,A)} \tag{2}$$

The Gini index is used to measure the partitioning complexity applied by feature A while contributing information gain IG, where SplitInfo is the splitting information. The decrease in the Gini index is expressed as:

$$\Delta\text{Gini}(S,A) = \text{Gini}(S) - \sum_{v\in\text{Values}(A)} \frac{|S_v|}{|S|}\text{Gini}(S_v) \tag{3}$$

The decrease in the Gini index characterizes the reduction in the impurity of node data after splitting through feature A, where Gini(S) is expressed as:

$$\text{Gini}(S) = 1 - \sum_{i=1}^{c} p_i^2 \tag{4}$$

This equation represents the proportion of category i in node S. The final hybrid split score is computed as a weighted sum of the normalized IGR and Gini decrease (Equation 5).

$$\begin{aligned}\text{HybridScore}(S,A) =& \alpha \cdot \frac{\text{GainRatio}(S,A)}{\text{MaxGR}} \\ &+ (1-\alpha)\cdot\frac{\Delta\text{Gini}(S,A)}{\text{Max}\Delta\text{Gini}}\end{aligned} \tag{5}$$

In equation (5), MaxGR and MaxΔGini represent the maximum values of the information gain ratio and Gini index decrease for all candidate features at the current node, respectively, used for normalization. While Information Gain Ratio (IGR) and Gini Index are both impurity measures, they exhibit complementary biases: IGR favors features with fewer distinct values, whereas Gini is less influenced by value cardinality and more sensitive to class probability changes. In physiological data, features like LF/HF ratio are continuous, while others like SCR peak counts are discrete with varying scales. A dynamic hybrid criterion allows the model to adaptively balance these biases based on node purity: prioritizing IGR for clearer separation (higher purity) to avoid over-partitioning, and leaning on Gini in mixed nodes to capture probability shifts. This adaptability addresses the limitations of using a single, fixed criterion across all splits in a complex feature space. For any continuous feature, the model determines the optimal splitting threshold θ that maximizes HybridScore(S,A) by iterating through all its possible values. The weighting coefficient α dynamically adjusts based on data purity Purity(S) of node S (Equation 6). This design prioritizes IGR in purer nodes for clearer splits and relies more on Gini in mixed nodes to capture class probability shifts.

$$\alpha = 1 - \text{Purity}(S)^{\beta} \tag{6}$$

In equation (6), β is a hyperparameter for adjusting sensitivity. This design makes it more inclined to use the Gini index to improve efficiency in nodes with relatively pure data, while relying more on the information gain ratio to enhance discrimination ability in nodes with more mixed data. The model adopts a pre-pruning strategy to control complexity and uses cross-validation to determine the optimal hyperparameter β and the minimum number of leaf node samples [28,29]. The complete algorithm execution flow is shown in Figure 2. The enhanced decision tree technique is depicted in Figure 2, demonstrating the primary decision-making process and unique process of the proposed method for multimodal physiological feature data. The decision tree begins developing by initiating the construction with a root node with all multimodal physiological feature data. The major point of innovation relates to the splitting of each non-leaf node. The proposed system does not use a single measurement criteria but implements a dynamically weighted hybrid splitting submodule. The hybrid splitting submodel determines the information gain ratio and Gini index decrease of each candidate feature during each split in parallel, and then calculates the fusion weight dynamically based on the purity of the data in the current node to ultimately produce a hybrid splitting score which takes advantage of the two measurement criteria. Then the splitting node selects the feature which is most discriminative to split the node based on the calculated score from the hybrid splitting sub-module. The sample path shown in the figure indicates that as the splitting feature of the root node, the system may choose to split the node first using the LF/HF ratio, and subsequently would route the data flow in various branches based on the threshold selected. The subsequent nodes are further split by some number of features such as skin conductance response peak values, which will ultimately stop at the leaf nodes representing "calm", "moderate stress", or "high stress," and "empathic distress". This structure intuitively illustrates a mapping path from raw physiological signals to discrete psychological states, but importantly, it illustrates how the improved splitting criterion improves the ability to adaptively balance the information content and purity of features at important nodes, yielding improved accuracy and robustness in psychological state classification, thus ensuring high accuracy and explainability in the model.

D. REAL-TIME PSYCHOLOGICAL CARE INTERVENTION MECHANISM BASED ON IDENTIFICATION

Once the psychological state category outputted by the decision tree model designates a corresponding personalized tactile intervention strategy, the proposed model uses a given mapping function defined mathematically as follows:

$$I = f(C, I_{\text{profile}}) \tag{7}$$

In equation (7), C denotes the discrete psychological state category, as inferred by the decision tree model, and I_{profile} is the set of individual intervention parameters that have been predetermined. The tactile feedback mode can be defined as having three parameters: intensity of vibration, frequency of vibration, and the pattern of intermittent pulse. In the identified psychological state with the categorical label "high stress," the vibration mode is to be high-intensity, low-frequency continuous vibration and the individual parameters that are to be used for the feedback modes are to be defined by the baseline comfort threshold A_{base} and the adjustment coefficient k_A in the I_{profile}, specifically as follows:

$$A = A_{\text{base}} \cdot k_A, \quad k_A > 1 \tag{8}$$

This pattern of continuous vibration is high-intensity and low-frequency, and aims to distract the user of cognitive load while also cutting off stress responses through significant somatic sensory input. For the "empathic distress" state, the pattern consists of a moderate-intensity vibrating pulse rhythmic pattern that is approximately equivalent to the resting heart rate of a human, and this patterned pulse is modified using the equation (9):

$$F = F_{\text{rest}} \pm \Delta F \tag{9}$$

where F_{rest} refers to the resting heart rate of the user (while making a small adjustment denoted by ΔF). The physiological outcome is to help bring the user's breathing rate and heart rate into sync with the pulse as a means of calming and self-regulating their emotions. All intervention instructions are sent from the host application to the microcontroller using a serial communication protocol to instruct the linear resonant actuator to provide a meaningful and patterned tactile feedback, creating an automated closed loop intervention circuit from perception of state to regulation of physiology.

III. EXPERIMENTAL DESIGN

A. EXPERIMENTAL SCENARIO

To evaluate the effectiveness of the system, it ran the experiment at a high-fidelity medical simulation center that closely mimicked a real-life clinical setting. The design of the scenarios centered on two highly emotional-load medical humanities situations: end-of-life care and discussing the diagnosis of complicated diseases. Both scenarios had rigorously trained standardized patients and were executed from standardized medical communication scripts to provide rigour to the experiment.

A total of 58 third- to fourth-year clinical medical students participated in the study, resulting in 31 male and 27 female participants, with an average age of about 22. None of the participants reported any current episodes of cardiovascular or dermatological diseases, and none had consumed caffeine, alcohol, or any medications affecting the autonomic nervous system within 24 hours prior to participating in the experiment. The experimental protocol received was approved by the Ethics Committee of Hebi Polytechnic, and all subjects prior to participation signed written informed consent documents. The experiment employed a within-subjects design where each of the 58 subjects completed simulated communication tasks sequentially in both scenarios while using data collection during the entire experiment via the intelligent clothing system described in this document.

B. DATA ACQUISITION PROCESS AND LABELING

Data collection was conducted alongside the subjects' engagement in the standardized simulated communication task. The intelligent clothing system continuously measured raw electrocardiogram and skin conductance signals, while two high-definition cameras located within the experimental room recorded documented video images of facial expressions and full body behavior. All data streams were synchronized to a centralized server via the laboratory's internal network, and the recording was synchronized with millisecond-level precision through the use of timecode. Upon signal acquisition, a labeling team of three psychologists with designated registered supervisor status within the Chinese Psychological Society's Clinical Psychology Registration System, labeled data according to a specified, standardized protocol. The labeling process identified intervals of thirty seconds as the basic unit for data analysis. To ensure that the ground truth labels were independent of the physiological features used for model training, the labeling process was primarily based on the behavioral video footage. Each labeler independently viewed the video clips and assigned a psychological state label according to the behavioral indicators defined in Table 2. The synchronized physiological data

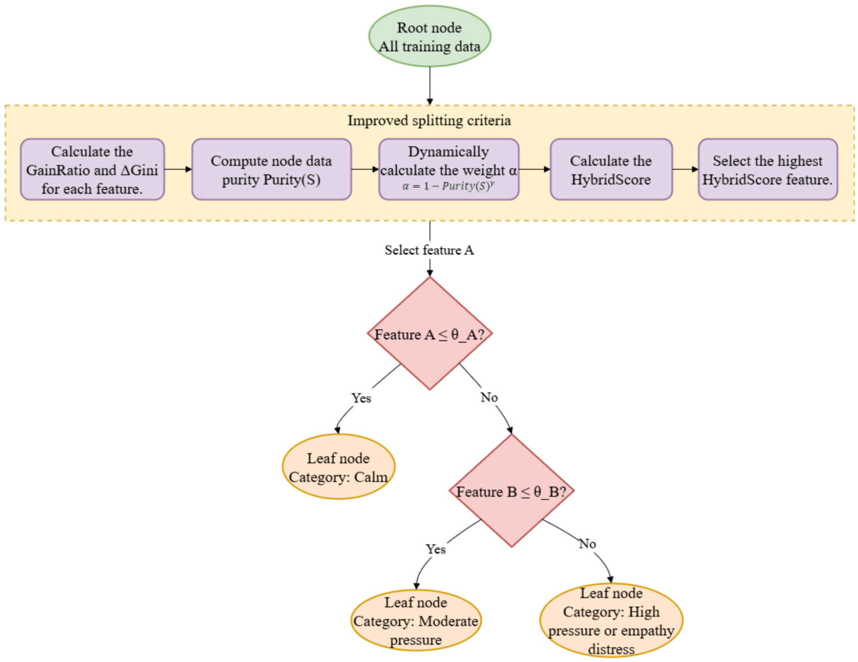

FIGURE 2. Decision tree model algorithm flow

stream was only accessible during a subsequent consistency review phase, where it was used sparingly by the experts to resolve ambiguous cases where behavioral cues were insufficient (e.g., subtle facial expressions). This protocol ensured that the final labels were behaviorally anchored and not directly inferred from the physiological patterns the model was intended to learn. The final labeling system and definitions of operation are displayed in Table 2.

TABLE 2. Psychological State Labeling System and Operational Definitions

Psychological state label	Primary behavioral indicators	Typical physiological response patterns
Calm	Natural expression, steady tone, coordinated body movements	HRV LF/HF ratio within individual baseline range, stable skin conductance level
Moderate stress	Increased speech rate, few repetitive gestures, reduced eye contact	LF/HF ratio increased by 50%-150% from baseline, discrete skin conductance response peaks appear
High stress	Significant decline in verbal fluency, body stiffness, noticeable self-soothing touches	LF/HF ratio persistently >150% above baseline, frequent and significant skin conductance response peaks
Empathic distress	Prolonged silence, avoidance of eye contact, facial expressions of pain or contemplation	Significant heart rate deceleration, accompanied by slow, persistent rise in skin conductance level

This labeling system creates a multimodal assessment standard from outward behaviors and internal physiological measures. It is crucial to note the operational distinction between ‘Empathic Distress’ and ‘High Stress’ at the physiological level. While both may involve elevated arousal, ‘Empathic Distress’ is defined by a specific autonomic co-activation pattern: it combines heart rate deceleration (often reflecting a parasympathetic ‘freezing’ or withdrawal response) with a slow, persistent rise in skin conductance level (SCL), representing sustained, low-grade sympathetic arousal. In contrast, ‘High Stress’ is characterized by a sympathetic-dominant ‘fight-or-flight’ pattern, typified by heart rate acceleration, a high LF/HF ratio, and frequent, phasic skin conductance responses (SCR peaks). This distinct physiological signature provides the basis for algorithmic discrimination. Behavioral measures provide intuitive, contextualized, qualitative data for identifying states of interest, while the pattern of physiological responses provides objective data that is quantifiable. Together they offer a strong basis for labeling matters and provide scientific consistency in the measurement of psychological states. Inter-labeling reliability is determined by calculating the Cohen’s Kappa coefficient and indicates good consistency in the results of the labeling [30,31].

C. BASELINE METHODS AND PARAMETER SETTINGS

To objectively evaluate the performance of the improved decision tree model proposed in this paper, three representative machine learning algorithms were selected as baseline comparison methods: standard C4.5 decision tree, support vector machine, and random forest [32,33]. All models used the same preprocessed multimodal physiological feature vectors as input and were designed for the same four-class mental state recognition task.

The standard C4.5 decision tree uses information gain ratio as the splitting criterion, the support vector machine uses radial basis function as kernel function, and the random forest is an ensemble of 100 decision trees. The improved decision tree model proposed in this paper applies the dynamic weighted hybrid splitting criterion mentioned above. The hyperparameters of all models, including regularization coefficients, kernel function parameters, maximum tree depth, and minimum number of leaf node samples, are optimized on the validation set through grid search combined with five-fold cross-validation [34,35]. The optimal parameter configurations of each model are shown in Table 3.

TABLE 3. Model Hyperparameter Configuration

Model	Hyperparameter	Value
Standard C4.5	Pruning cofidence	0.25
Standard C4.5	Minimum instances per leaf	2
SVM (Support Vector Machine)	Kernel	RBF
SVM (Support Vector Machine)	Regularization parameter (C)	10
SVM (Support Vector Machine)	Kernel coefficient	0.1
Random forest	Number of trees	100
Random forest	Maximum depth	15
Random forest	Features per split	sqrt
Proposed model	Hybrid weight coefficient	1.5
Proposed model	Minimum instances per leaf	3

Table 3 shows the parameter configurations, reflecting the inherent requirements of different model algorithms and their adaptation to data characteristics. Standard C4.5 employs a relatively aggressive pruning confidence level to control overfitting; the parameters of Support Vector Machines and Random Forests reflect their balance between model complexity and generalization ability when handling nonlinear physiological characteristics; while the weight coefficients unique to the model in this paper are greater than 1, indicating that its splitting strategy is more sensitive to changes in node purity and tends to retain the dominant role of information gain rate in more nodes, which aligns with the design goal of improving model discrimination accuracy. A unified parameter optimization process ensures that all comparison models are performed under their respective optimal configurations.

IV. EXPERIMENTAL RESULTS AND ANALYSIS

A. COMPARATIVE ANALYSIS OF MODEL MENTAL STATE RECOGNITION PERFORMANCE

To evaluate the generalization ability and robustness of the improved decision tree model in different highemotional-load medical scenarios, this study systematically compared the classification performance of the proposed model with three mainstream baseline methods in two typical scenarios: end-of-life care and complex diagnosis. Based on the same multimodal physiological feature dataset, this analysis used four core metrics—accuracy, precision, recall, and F1 score—to measure the actual effectiveness of each model in complex real-world teaching environments. The scenario-specific performance comparison results are shown in Figure 3.

Figure 3 illustrates the performance differences of each model in the two experimental scenarios. Subplot a corresponds to the end-of-life care scenario, and subplot b corresponds to the difficult-to-diagnose scenario. The horizontal axis represents the four comparative models, and the vertical axis represents the percentage of performance indicators. Data shows that the improved decision tree model proposed in this paper achieves the optimal performance in both scenarios. Its accuracy in the end-of-life care scenario reaches 93.5%, an improvement of 2.7 percentage points compared to the second-best performing random forest; its accuracy in the difficult-to-diagnose scenario is 91.8%, also leading the random forest by 3.7 percentage points. All models show a systematic decline in performance in the difficult-to-diagnose scenario. The accuracy of the standard C4.5 drops from 86.5% to 83.8%, and the F1 score of the support vector machine drops from 88.2% to 85.2%. This phenomenon stems from the more complex emotional interplay and higher cognitive load in the difficult-to-diagnose situation, leading to more ambiguous and variable physiological representations of psychological states, increasing the difficulty of classification. The model presented in this paper, with its dynamically weighted hybrid splitting criterion, can adaptively adjust the feature selection strategy, thereby maintaining relatively high discrimination accuracy in more challenging scenarios, and verifying its effectiveness and robustness in the complex application environment of medical humanities education.

B. IN-DEPTH ANALYSIS OF THE EFFECTIVENESS OF PSYCHOLOGICAL STATE DISCRIMINATION IN DIFFERENT SCENARIOS

In order to explore the discriminatory attributes and constraints of the enhanced decision tree model across different contexts in medical humanities, this study presented analyses of the classification features of the model under three conditions (overall data, end-of-life care, and difficult diagnosis). This analysis through a multi-scenario confusion matrix, systematically evaluated the discriminatory preferences and confusion in each condition of the model across four psychological state types, and hoped to uncover situational factors' impact on distinguishability of the physiological implementations of psychological states. The detailed distribution of classification efficacy is shown in Figure 4.

Figure 4 shows the classification results of the model across different data ranges. The horizontal axis represents the psychological state labels predicted by the model, and the vertical axis represents the actual psychological state labels. The color depth and value of each cell represent the percentage of the corresponding category pair that was correctly identified. In the end-of-life care scenario, the model achieved an 87.7% recognition rate for the empathic distress state, significantly higher than the 79.9% in the difficult diagnosis scenario. Simultaneously, the proportion of empathic distress states misclassified as high stress in the

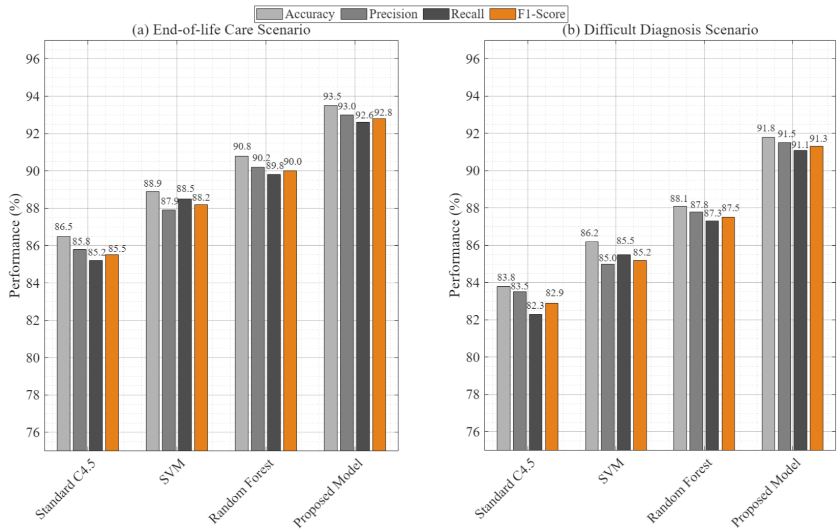

FIGURE 3. Classification performance comparison results: (a) End-of-life care scenario; (b) Difficult diagnosis scenario

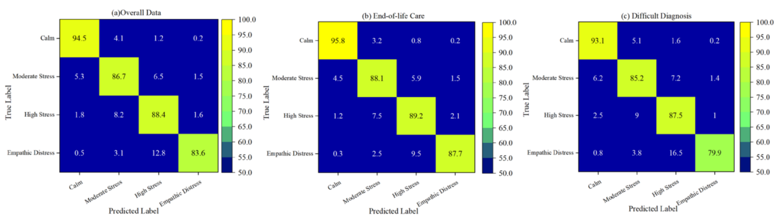

FIGURE 4. Confusion matrix of psychological states in different scenarios: (a) Overall data confusion matrix; (b) Confusion matrix for end-of-life care scenarios; (c) Confusion matrix for complex diagnosis scenarios

difficult diagnosis scenario reached 16.5%, higher than the 9.5% in the end-of-life care scenario. This difference stems from the different emotional induction mechanisms of the two scenarios: the emotional response evoked in the end-of-life care scenario is purer and primarily characterized by sadness and pity, with a higher degree of distinction between its physiological patterns and stress states; while the difficult diagnosis scenario mixes high cognitive load and emotional conflict, leading to a significant overlap in the physiological representations of empathic distress and high stress, both manifesting as increased sympathetic nerve activation and decreased heart rate variability. The model exhibited the best consistency in identifying the calm state, indicated by a 94.5% overall accuracy with the dataset used in this study. In this case, it was more measurable because the physiological pattern features of the calm state are distinct, and the boundaries of distinction between the calm state and the other states are sharper. The analysis results demonstrated a clear effect of situational features on the accuracy of mental state recognition, and the complex influence from emotional and cognitive layers makes distinguishing between states more challenging.

C. SCENARIO DEPENDENCY ANALYSIS OF KEY DECISION PATHS

To illustrate the adaptive alteration of the improved decision tree model's decision-making logic in different medical humanities contexts, this study extracted and compared the critical decision paths of the model in identifying high-stress states during end-of-life care and in the context of a difficult diagnosis. The analysis will attempt to show how, and in what ways, the model dynamically adapts dependent physiological characteristics, as well as decision thresholds, based on the features of the context in order to derive a deeper understanding of how the model works internally and the specificity of context. The comparison of the decision-making paths of the model is presented in Figure 5.

Figure 5 depicts the typical decision paths in two scenarios. In the end-of-life care scenario, the model starts off using an LF/HF ratio of 2.35 as the root node split threshold to screen for high arousal samples. Then it uses the mean peak frequency of skin conductance response (SCR) at 6 times per minute to use as secondary judgement criterion to identify states of high stress with 92% purity overall. This path indicates that high stress in the end-of-life care scenario is evidenced primarily by an episodic activation of the sympathetic nervous system. In contrast, the decision-making path in the difficult-to-diagnose scenario reveals

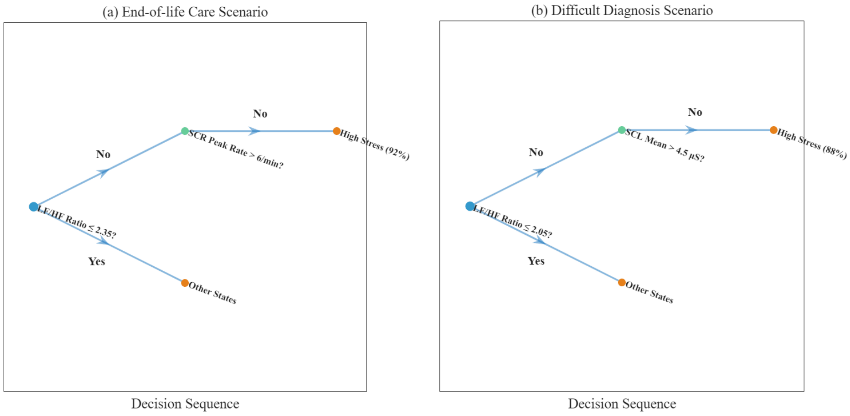

FIGURE 5. Comparison of Decision Paths: (a) End-of-life care scenario; (b) Difficult diagnosis scenario

distinctly different features: the root node relies on a more conservative LF/HF ratio threshold of 2.05 and is reflective of the higher, overall physiological arousal in the scenario; secondary decision-making relies on sustained mean skin conductance level (SCL) rather than existing peaks, using a threshold of 4.5 μS and was associated with lower purity of 88% overall. This difference in decision paths is due to the continuous interaction of cognitive load and emotional stress in the difficult-to-diagnose scenario that resulted in a more stable, and sustained increase in physiological responses to high stress as opposed to bursts indicated by peak responses. The scenario-dependent nature of the decision path confirms that the model can adaptively capture the specific physiological representations of psychological states in different situations, and its discrimination logic is consistent with the theoretical expectation in clinical psychology that different stressors trigger differentiated physiological responses.

D. EVALUATION OF PHYSIOLOGICAL EVIDENCE FOR THE EFFECTIVENESS OF PSYCHOLOGICAL CARE INTERVENTION

To quantitatively evaluate the physiological regulatory effect of personalized tactile intervention on specific psychological states in different medical humanities contexts, this study systematically analyzed the changes in the LF/HF ratio before and after intervention in two scenarios: end-of-life care and difficult diagnosis, which showed high stress and empathic distress. This revealed whether the regulatory effect of intervention on sympathetic-vagal balance was modulated by both situational characteristics and psychological state type. The scenario-specific intervention effects were compared in Figure 6.

Figure 6 shows the distribution of the LF/HF ratio before and after intervention under four experimental conditions. The horizontal axis clearly indicates the combination of scenarios and states, and the vertical axis represents the LF/HF ratio, a key indicator of sympathetic nerve activity. In the high-stress state of the end-of-life care scenario, the intervention reduced the LF/HF ratio from the median of 3.85 to 2.10, a decrease of 45.5%; while in the same scenario, the empathic distress state decreased from 2.90 to 1.95, a decrease of 32.8%. The high-stress state of the difficult diagnosis scenario showed the largest absolute decrease, with the LF/HF ratio decreasing from 4.40 to 2.35, a reduction of 46.6%; the empathic distress state in this scenario decreased from 3.10 to 2.20, a reduction of 29.0%. The differences in intervention effects stem from the inherent differences in autonomic nerve response patterns under different scenarios: the high-stress state in the difficult diagnosis scenario is accompanied by the strongest sympathetic nerve activation, and the pre-intervention baseline provides a larger adjustment space for intervention measures; the empathic distress state shows a relatively mild physiological response in both scenarios, and its intervention effect is correspondingly weaker. All conditions reached statistical significance, confirming that tactile intervention can effectively promote the recovery of sympathetic nerve activity to a balanced state. The strength of the effect is jointly influenced by the initial arousal level and situational characteristics, with high sympathetic activation states benefiting more significantly from the intervention.

E. CONSISTENCY OF SCENARIOS IN THE CORRELATION BETWEEN SUBJECTIVE EXPERIENCE AND OBJECTIVE RECOGNITION

To verify the psychological validity of the system's identification results and its robustness across different medical humanities contexts, this study examined the association pattern between the stress level automatically identified by the system and the changes in subjects' self-reported anxiety states. This analysis quantified the consistency between objective physiological identification and subjective psychological experience across different scenarios using linear regression, aiming to confirm the clinical significance and cross-scenario applicability of the system's output. The comparison of the association patterns is shown in Figure 7.

Figure 7 illustrates the correlation between systemic recognition stress levels and changes in STAI (State-Trait Anxiety Inventory) scores in two scenarios using scatter

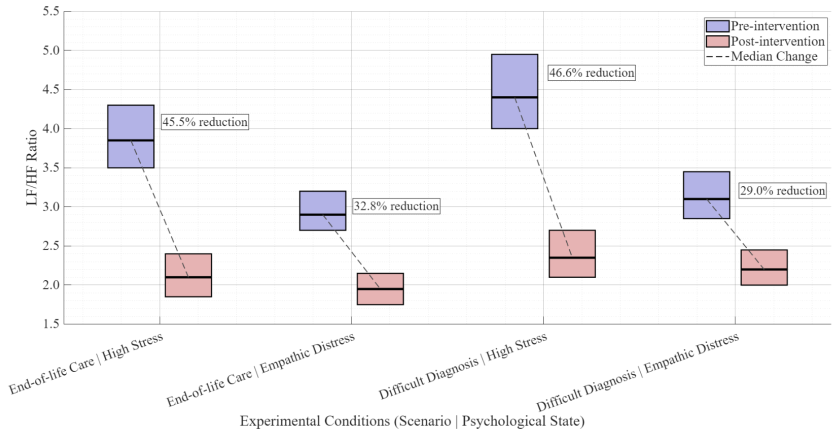

FIGURE 6. Intervention effects under different experimental conditions

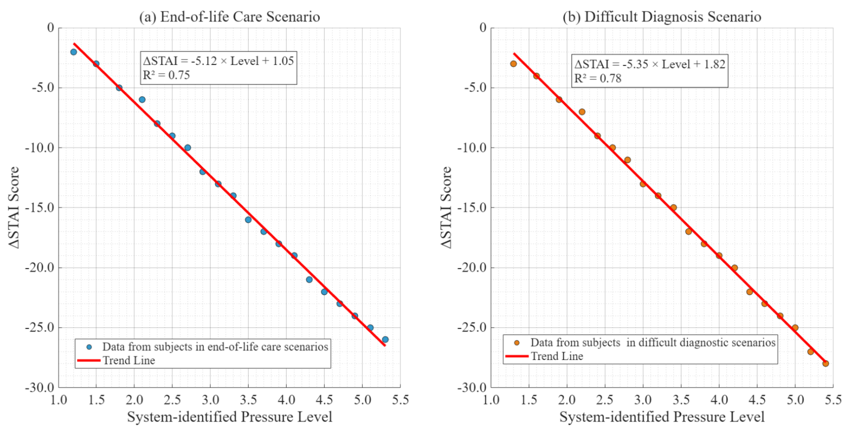

FIGURE 7. Comparison of Association Patterns: (a) End-of-life care scenario; (b) Difficult diagnosis scenario

plots and fitted curves. In the end-of-life care scenario, the regression equation is $\Delta STAI = -5.12 \times Level + 1.05$, with a coefficient of determination (R^2) of 0.75; in the difficult diagnosis scenario, the regression equation is $\Delta STAI = -5.35 \times Level + 1.82$, with an R^2 of 0.78. A significant negative correlation is observed in both scenarios. For every unit increase in systemic recognition stress level, subjects' STAI scores decrease by an average of 5.12 points in the end-of-life care scenario and 5.35 points in the difficult diagnosis scenario. The slopes of the two regression equations are highly similar, with a difference of only 0.23, indicating that the strength of the association between systemic recognition and subjective experience remains stable across different situations. This consistency across scenarios results from shared autonomic neural underpinnings of physiological indicators (LF/HF ratio and skin conductance response) on which the system is dependent, as well as the unmodified nature by particular situational meanings of their association patterns. Both scenarios achieved statistical significance and had a determination coefficient higher than 0.70, demonstrating that the system's identification results have solid psychological validity and can reliably reflect the subjects' true subjective emotional experiences. Its association patterns have good consistency and universality in different medical humanities contexts.

V. CONCLUSION

This study demonstrates the viability of smart textile systems based on an improved decision tree algorithm, enabling real-time and accurate identification and personalized intervention of the psychological state of students in medical humanities education. The system integrates flexible sensors to collect multimodal physiological signals such as heart rate variability and skin conductance, and optimizes the decision tree model using a dynamically weighted hybrid splitting criterion, effectively improving the accuracy and interpretability of psychological state discrimination. Experimental results show that the system achieves recognition accuracy of 93.5 % and 91.8 % in two typical scenarios: end-of-life care and difficult diagnosis. In the end-of-life care scenario, using an LF/HF ratio of 2.35 as the root node splitting threshold, the highest purity for identifying high-stress states is 92%. In the difficult diagnosis scenario, the LF/HF ratio decreased by 46.6% after intervention in the high-stress state. The system's observation findings are also significantly consistent with subjective anxiety experiences, with a coefficient of determination R^2=0.78 in the difficult diagnosis scenario, corroborating the psychological validity of its output. Here, this approach permits objective yet quantitative-level detection of emotional experiences for purposes of psychological care in medical humanities education via a closed-loop (perception-decision-intervention) based method that alleviates the limitations of older book-ending review methods that are subjective and do not allow for real-time access. Accordingly, it has great value to educators as it can easily be integrated into clinical skills training environments, allowing educators to monitor students' emotional states dynamically, while providing a technical avenue for robustly enacting precise teaching interventions and emotional support and presenting clear application value for enhancing the work of students' humanistic education.

AUTHOR CONTRIBUTIONS

This article has only one author. The author is solely responsible for all aspects of this work, including study conception, design, execution, analysis, and manuscript preparation.

FUNDING

This work was supported by Henan Medical Education Research Project (Project No.: WJLX2024127): Application Research of Virtual Simulation Platform in Rehabilitation Department Internship Teaching under the OBE Concept.

CONFLICTS OF INTEREST

The author affirm that he does not have any financial conflicts of interest.

HUMAN RESEARCH SUBJECTS

The experimental protocol received Hebi Polytechnic ethics review committee approval, and all subjects prior to participation signed written informed consent documents.

DATA AVAILABILITY STATEMENT

The data that support the findings of this study are available from the corresponding author, upon request.

ACKNOWLEDGEMENTS

Not applicable.

REFERENCES

[1] C. C. Behrens, E. W. Driessen, D. H. Dolmans, and G. J. Gormley, "'A roller coaster of emotions': A phenomenological study on medical students lived experiences of emotions in complex simulation," Advances in Simulation, vol. 6, no. 1, pp. 24, 2021, doi: 10.1186/s41077-021-00177-x.

[2] H. L. Lin, Y. C. Wang, M. L. Huang, N. W. Yu, I. Tang, Y. C. Hsu, et al., "Can virtual reality technology be used for empathy education in medical students: A randomized case-control study," BMC Medical Education, vol. 24, no. 1, pp. 1254, 2024, doi: 10.1186/s12909-024-06009-6.

[3] A. Rajagopalan, Q. H. Chew, and K. Sim, "Medical Humanities in Undergraduate Psychiatry Teaching: Learner Assessment and Mediators of Better Learning Outcomes," Journal of Medical Education and Curricular Development, vol. 10, Art. no. 23821205231214393, 2023, doi: 2071-1050/16/14/6080.

[4] J. Graves, E. Flynn, R. Woodward-Kron, and W. C. Hu, "Supporting medical students to support peers: A qualitative interview study," BMC Medical Education, vol. 22, no. 1, pp. 300, 2022, doi: 10.1186/s12909-022-03368-w.

[5] K. Sattar, M. S. B. Yusoff, W. N. Arifin, M. A. M. Yasin, and M. Z. M. Nor, "Effective coping strategies utilised by medical students for mental health disorders during undergraduate medical education-a scoping review," BMC medical education, vol. 22, no. 1, pp. 121, 2022, doi: 10.1186/s12909-022-03185-1.

[6] J. R. Winkler and M. Appel, "Measuring dynamic emotional experiences in response to media stimuli," Frontiers in Psychology, vol. 15, Art. no. 1436918, 2024, doi: 10.3389/fpsyg.2024.1436918.

[7] V. Coronado-Vázquez, C. Antón-Rodríguez, J. Gómez-Salgado, M. D. V. Ramírez-Durán, and S. Álvarez-Montero, "Evaluation of learning outcomes of humanities curricula in medical students," A meta-review of narrative and systematic reviews. Frontiers in Medicine, vol. 10, Art. no. 1145889, 2023, doi: 10.3389/fmed.2023.1145889.

[8] P. Barbadoro, A. Brunzini, J. Dolcini, M. D. V. Ramírez-Durán, and S. Álvarez-Montero, "Stress responses in highfidelity simulation and standard simulation training among medical students," BMC Medical Education, vol. 23, no. 1, pp. 116, 2023, doi: 10.3389/fmed.2023.1145889.

[9] J. Isaksson, J. Krabbe, and M. Ramklint, "Medical students' experiences of working with simulated patients in challenging communication training," Advances in Simulation, vol. 7, no. 1, pp. 32, 2022, doi: 10.1186/s41077-022-00230-3.

[10] Z. Zhang, J. M. Fort, and L. Giménez Mateu, "Facial expression recognition in virtual reality environments: Challenges and opportunities," Frontiers in Psychology, vol. 14, Art. no. 1280136, 2023, doi: 10.3389/fpsyg.2023.1280136.

[11] Y. Cai, X. Li, and J. Li, "Emotion recognition using different sensors, emotion models, methods and datasets: A comprehensive review," Sensors, vol. 23, no. 5, pp. 2455, 2023, doi: 10.3390/s23052455.

[12] B. A. Hickey, T. Chalmers, P. Newton, C. T. Lin, D. Sibbritt, C. S. McLachlan, et al., "Smart devices and wearable technologies to detect and monitor mental health conditions and stress: A systematic review," Sensors, vol. 21, no. 10, pp. 3461, 2021, doi: 10.3390/s21103461.

[13] E. Müller, I. Benke, and A. Maedche, "Heart Rate-Based Emotion Recognition and Adaptive Emotion Regulation Support with Wrist-Worn Wearables: A Systematic Literature Review," NeuroIS Retreat, vol. 68, pp. 355-366, 2023, doi: 10.1007/978-3-031-58396-4_31.

[14] Z. Li, Y. Xing, Y. Pi, M. Jiang, and L. Zhang, "A novel physiological feature selection method for emotional stress assessment based on emotional state transition," Frontiers in Neuroscience, vol. 17, Art. no. 1138091, 2023, doi: 10.3389/fnins.2023.1138091.

[15] R. Guo, H. Guo, L. Wang, M. Chen, D. Yang, and B. Li, "Development and application of emotion recognition technology—a systematic literature review," BMC Psychology, vol. 12, no. 1, pp. 95, 2024, doi: 10.1186/s40359-024-01581-4.

[16] S. Fernandes, A. Ramos, M. Vega-Barbas, C. García-Vázquez, F. Seoane, and I. Pau, "Smart Textile Technology for the Monitoring of Mental Health," Sensors, vol. 25, no. 4, pp. 1148, 2025, doi: 10.3390/s25041148.

[17] A. E. Avanu and G. Dodi, "Wear your heart on your sleeve: Smart textile ECG wearables for comfort, integration, signal quality and continuous monitoring in paroxysmal atrial fibrillation," Sensors, vol. 25, no. 3, pp. 676, 2025, doi: 10.3390/s25030676.

[18] D. Zhai, X. Bao, X. Long, T. Ru, and G. Zhou, "Precise detection and localization of R-peaks from ECG signals," Mathematical Biosciences and Engineering, vol. 20, no. 11, pp. 19191-19208, 2023, doi: 10.3934/mbe.2023848.

[19] A. F. Ahmed, "A novel improved Pan-Tompkins method for QRS complex detection of the ECG signal," Signal, Image and Video Processing, vol. 19, no. 12, pp. 960, 2025, doi: 10.1007/s11760-025-04587-6.

[20] M. Ramzan and S. Dawn, "Analyzing and identifying oscillatory activities of emotions based on Electroencephalography signals using power spectral density and spatial filtering techniques," Biomedical Signal Processing and Control, vol. 71, Art. no. 103193, 2022, doi: 10.1016/j.bspc.2021.103193.

[21] X. Li, Y. X. Dong, and F. L. Zhang, "Fully automated operational modal identification based on scale-space peak picking algorithm and power spectral density estimation," Measurement Science and Technology, vol. 35, no. 7, Art. no. 76206, 2024, doi: 10.1088/1361-6501/ad3a8d.

[22] A. M. Nelushi, C. H. Manathunga, N. G. S. Shantha Gamage, and T. Nakayama, "Assessing Cardiac Sympatho-Vagal Balance Through Wavelet Transform Analysis of Heart Rate Variability," Applied Sciences, vol. 15, no. 4, pp. 1687, 2025, doi: 10.3390/app15041687.

[23] A. S. Menezes Junior, A. A. Schröder, S. M. Botelho, and A. L. Resende, "Cardiac autonomic function in long COVID-19 using heart rate variability: An observational cross-sectional study," Journal of Clinical Medicine, vol. 12, no. 1, pp. 100, 2022, doi: 10.3390/jcm12010100.

[24] F. Aaboub, H. Chamlal, and T. Ouaderhman, "Statistical analysis of various splitting criteria for decision trees," Journal of Algorithms & Computational Technology, vol. 17, Art. no. 17483026231198181, 2023, doi: 10.1177/17483026231198181.

[25] V. G. Costa and C. E. Pedreira, "Recent advances in decision trees: An updated survey," Artificial Intelligence Review, vol. 56, no. 5, pp. 4765-4800, 2023, doi: 10.1007/s10462-022-10275-5.

[26] J. Yan, Z. Zhang, and H. Dong, "AdaDT: An adaptive decision tree for addressing local class imbalance based on multiple split criteria," Applied Intelligence, vol. 51, no. 7, pp. 4744-4761, 2021, doi: 10.1007/s10489-020-02061-z.

[27] M. Arifuzzaman, M. R. Hasan, T. J. Toma, S. B. Hassan, and A. K. Paul, "An advanced decision tree-based deep neural network in nonlinear data classification," Technologies, vol. 11, no. 1, pp. 24, 2023, doi: 10.3390/technologies11010024.

[28] Y. Zhang, Y. Xin, and Q. Li, "Research on parameter selection and optimization of C4," 5 algorithm based on algorithm applicability knowledge base. Scientific Reports, vol. 15, no. 1, Art. no. 29418, 2025, doi: 10.1038/s41598-025-11901-2.

[29] S. Buschjäger and K. Morik, "Joint leaf-refinement and ensemble pruning through L 1 regularization," Data Mining and Knowledge Discovery, vol. 37, no. 3, pp. 1230-1261, 2023, doi: 10.1007/s10618-023-00921-z.

[30] B. Więckowska, K. B. Kubiak, P. Jóźwiak, W. Moryson, and B. Stawińska-Witoszyńska, "Cohen's kappa coefficient as a measure to assess classification improvement following the addition of a new marker to a regression model," International Journal of Environmental Research and Public Health, vol. 19, no. 16, Art. no. 10213, 2022, doi: 10.3390/ijerph191610213.

[31] A. A. Chamid and R. Kusumaningrum, "Labeling consistency test of multi-label data for aspect and sentiment classification using the cohen kappa method," Ingenierie des Systemes d'Information, vol. 29, no. 1, pp. 161, 2024, doi: 10.18280/isi.290118.

[32] S. W. Purnami, S. Karimah, S. Andari, D. P. Wulandari, Y. S. Hadiwidodo, W. R. Islamiyah, et al., "Mental state classification based on electroencephalogram (EEG) using multiclass support vector machine," Medical Journal of Malaysia, vol. 80, no. 3, pp. 352-358, 2025.

[33] D. A. Fife and J. D'Onofrio, "Common, uncommon, and novel applications of random forest in psychological research," Behavior Research Methods, vol. 55, no. 5, pp. 2447-2466, 2023, doi: 10.3758/s13428-022-01901-9.

[34] Q. A. Hidayaturrohman and E. Hanada, "A Comparative Analysis of Hyper-Parameter Optimization Methods for Predicting Heart Failure Outcomes," Applied Sciences, vol. 15, no. 6, pp. 3393, 2025, doi: 10.3390/app15063393.

[35] A. G. Saputra, P. Purwanto, and P. Pujiono, "Hyperparameter Tuning Decision Tree and Recursive Feature Elimination Technique for Improved Chronic Kidney Disease Classification," Scientific Journal of Informatics, vol. 11, no. 3, pp. 821-830, 2024, doi: 10.15294/sji.v11i3.12990.